AIAA AVIATION Forum
June 27-July 1, 2022, Chicago, IL & Virtual
AIAA AVIATION 2022 Forum

10.2514/6.2022-3511

Equations of Motion for a Generic Multibody Tilt-rotor Aircraft

Jing Pei* and Carlos M. Roithmayr†
NASA Langley Research Center, Hampton, Virginia, 23681

A set of equations of motion for a generic tilt-rotor aircraft is presented. Equations governing the motion of the multibody vehicle are derived using Kane's method and shown in a compact form that is easily implemented. Contributions of aerodynamic and propulsive forces to the generalized active forces can be readily included. Simulation results presented for a four-rotor configuration illustrate the increased fidelity a multibody formulation provides compared to the traditional single-body approach.

I. Introduction

Electric vertical take-off and landing vehicles (eVTOL) have gained popularity recently in the emerging market of Urban Air Mobility (UAM). UAM vehicle configurations draw upon the advantages of traditional rotorcraft and fixed-wing aircraft. Fixed-wing aircraft offer longer endurance, better efficiency, and operations at high speeds, whereas rotorcraft have the ability to take off and land vertically, hover, and maneuver in confined space, as discussed in Ref. [1]. UAM vehicles are generally categorized into two types: tilt-wing (Refs. [1,2]) and tilt-rotor (Refs. [3–5]). Often in flight dynamic simulations, the vehicle is treated as a single rigid body; motion of individual rotors, nacelles, and wing sections relative to the fuselage is ignored. This approach can sometimes provide reasonably accurate results. However, when the mass and inertia of these appendages are significant compared to those of the main body, or appendages are moving at high relative speeds, or large motor torques are involved, it becomes necessary to simulate the dynamics of the multibody system. These dynamics must be well understood by the flight control engineer as they may adversely affect vehicle stability or handling qualities.

There appear to be three general categories of literature dealing with modeling and simulation of tilt-rotor aircraft. The first of these, exemplified by Refs. [6–8], involves an analytical single-rigid-body approach, where effects like rotor aerodynamics and blade flapping are treated with various levels of fidelity. In the second category, multibody models are implemented in commercial software, as presented in Refs. [9, 10]. These simulations are highly complex and involve hundreds of states, making it difficult to gain insight into the underlying dynamics of the vehicle. In the third category, where the present work belongs, an analytical multibody approach is taken. Reference [11] develops multibody equations using d'Alembert's principle. A majority of the details are withheld from the reader and a final set of equations is not provided. Reference [12] derives multibody equations for a two-rotor configuration using Newton's method; however, only the fuselage force and moment equations are provided. Reference [13] derives multibody equations for a two-rotor configuration using Kane's method. It is assumed that the two nacelles are tilted synchronously, allowing them to be modeled as one rigid body. A drawback of this approach is that the resulting equations cannot be used to simulate differential gimbaling of the nacelles, such as what is required to perform a yaw maneuver during hover. Motion of the rotors relative to the nacelles is not modeled; thus, the system consists of two rigid bodies having seven degrees of freedom. None of the aforementioned references establish the validity of the complex governing equations by checking for conservation of system angular momentum and kinetic energy.

The present work provides the reader with a set of detailed dynamical equations of motion that can be readily implemented and verified. Kane's method, as set forth in Ref. [15], is used in Sec. II to derive equations of motion for a generic tilt-rotor aircraft with n rotors. The multibody model accounts for independent,

*Aerospace Engineer, Atmospheric Flight Entry Systems Branch.
†Senior Aerospace Engineer, Vehicle Analysis Branch.

relative motion between each nacelle and the fuselage, and between each rotor and the nacelle to which it is connected. The system possesses $6+2n$ degrees of freedom. The equations are applied in Sec. III to a specific notional vehicle with four rotors and solved numerically for two cases. The first case serves as a check of the validity of the equations and the numerical solutions; conservation of system kinetic energy and angular momentum is demonstrated when the vehicle is not subject to external forces or the action of internal motors. The second case begins with the vehicle hovering. Motor torques are applied to tilt the nacelles forward, resulting in forward motion of the vehicle, and then the nacelles are returned to their original positions. In both cases the results of the multibody simulation are compared to those of a single-body simulation. Section IV summarizes the current work.

II. Dynamics

A. System Description

Figure 1 provides a notional example of a tilt-rotor aircraft with four rotors. A generic multibody vehicle is modeled as a rigid body B having mass m_B, together with n rigid, axisymmetric propellers $D_1, \ldots, D_n$, each of mass m_D. The mass center of the vehicle without propellers is denoted by $B^\star$ and the individual propeller mass centers are denoted by $D_i^\star$ $(i = 1, \ldots, n)$. A set of right-handed, mutually perpendicular unit vectors fixed in B is introduced such that $\hat{\mathbf{b}}_1$ is directed from the tail to the nose, $\hat{\mathbf{b}}_2$ is directed to the starboard wing, and $\hat{\mathbf{b}}_3$ completes the set. Each propeller is connected to B by two revolute joints. The first joint is parallel to $\hat{\mathbf{b}}_2$ and permits the nacelle, C_i, to move relative to B. The second joint is parallel to the propeller's axis of symmetry and permits the rotor to move relative to the nacelle. In this work, the mass and inertia of the nacelles are neglected. $D_i^\star$ is offset by a distance l_i from the axis of the first revolute joint. A set of right-handed, mutually perpendicular unit vectors fixed in reference frame C_i is introduced such that $\hat{\mathbf{c}}_2 = \hat{\mathbf{b}}_2$ is parallel to the first revolute joint and $\hat{\mathbf{c}}_1$, which has the same direction as the thrust force applied by the propeller, is parallel to the second revolute joint. Angular displacement of the first joint is denoted by the angle δ_i whereas the rotation of the propeller D_i relative to C_i is measured by an angle ϕ_i. (Strictly speaking, a subscript i should accompany unit vectors $\hat{\mathbf{c}}_1$, $\hat{\mathbf{c}}_2$, and $\hat{\mathbf{c}}_3$ but it is omitted for convenience.) Unit vectors fixed in B are related to those fixed in C_i by the direction cosine matrix in Table 1.

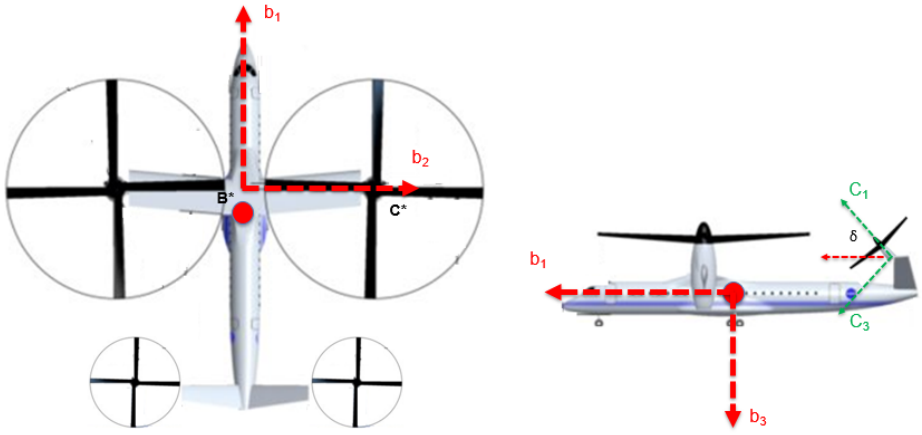

Figure 1. Notional tilt-rotor aircraft with four propellers (image credit: Ref. [14]).

Table 1. Direction cosine matrix

	$\hat{\mathbf{b}}_1$	$\hat{\mathbf{b}}_2$	$\hat{\mathbf{b}}_3$
$\hat{\mathbf{c}}_1$	$\cos\delta_i$	0	$-\sin\delta_i$
$\hat{\mathbf{c}}_2$	0	1	0
$\hat{\mathbf{c}}_3$	$\sin\delta_i$	0	$\cos\delta_i$

B. Velocities and Accelerations

The velocity ${}^N\mathbf{v}^{B^\star}$ of $B^\star$ in an inertial reference frame N is defined in terms of three motion variables u_1, u_2, and u_3, as

$$ {}^N\mathbf{v}^{B^\star} = u_1\hat{\mathbf{b}}_1 + u_2\hat{\mathbf{b}}_2 + u_3\hat{\mathbf{b}}_3 \tag{1}$$

The angular velocity ${}^N\boldsymbol{\omega}^{B}$ of B in N is defined in terms of motion variables u_4, u_5, and u_6, as

$$ {}^N\boldsymbol{\omega}^{B} = u_4\hat{\mathbf{b}}_1 + u_5\hat{\mathbf{b}}_2 + u_6\hat{\mathbf{b}}_3 \tag{2}$$

The angular velocity ${}^N\boldsymbol{\omega}^{C_i}$ of C_i in N is defined as

$$ {}^N\boldsymbol{\omega}^{C_i} = u_4\hat{\mathbf{b}}_1 + (u_5+u_{6+i})\hat{\mathbf{b}}_2 + u_6\hat{\mathbf{b}}_3 \qquad (i=1,\ldots,n) \tag{3}$$

where $u_{6+i} \triangleq \dot{\delta}_i$. The angular velocity ${}^N\boldsymbol{\omega}^{D_i}$ of D_i in N is defined as

$$ {}^N\boldsymbol{\omega}^{D_i} = u_4\hat{\mathbf{b}}_1 + (u_5+u_{6+i})\hat{\mathbf{b}}_2 + u_6\hat{\mathbf{b}}_3 + u_{6+n+i}\hat{\mathbf{c}}_1 \qquad (i=1,\ldots,n) \tag{4}$$

where $u_{6+n+i} \triangleq \dot{\phi}_i$. The angular momentum of B relative to $B^\star$ in N is given by

$$ {}^N\mathbf{H}^{B/B^\star} = \underline{\mathbf{I}}^{B/B^\star} \cdot {}^N\boldsymbol{\omega}^{B} \tag{5}$$

where $\underline{\mathbf{I}}^{B/B^\star}$ is the central inertia dyadic of B. The time derivative in N of ${}^N\mathbf{H}^{B/B^\star}$ is given by

$$ \frac{{}^N d\,{}^N\mathbf{H}^{B/B^\star}}{dt} = \underline{\mathbf{I}}^{B/B^\star} \cdot \frac{{}^B d\,{}^N\boldsymbol{\omega}^{B}}{dt} + {}^N\boldsymbol{\omega}^{B} \times \underline{\mathbf{I}}^{B/B^\star} \cdot {}^N\boldsymbol{\omega}^{B} \tag{6}$$

where ${}^N d/dt$ indicates differentiation with respect to time in N. The angular momentum of D_i relative to $D_i^\star$ in N is given by

$$ {}^N\mathbf{H}^{D_i/D_i^\star} = \underline{\mathbf{I}}^{D_i/D_i^\star} \cdot {}^N\boldsymbol{\omega}^{D_i} \qquad (i=1,\ldots,n) \tag{7}$$

where $\underline{\mathbf{I}}^{D_i/D_i^\star}$ is the central inertia dyadic of D_i. A set of right-handed, mutually perpendicular unit vectors $\hat{\mathbf{d}}_1$, $\hat{\mathbf{d}}_2$, and $\hat{\mathbf{d}}_3$ are fixed in D_i such that $\hat{\mathbf{d}}_1 = \hat{\mathbf{c}}_1$. Because D_i is axisymmetric, one may write $\underline{\mathbf{I}}^{D_i/D_i^\star} = I_s\hat{\mathbf{d}}_1\hat{\mathbf{d}}_1 + I_t(\hat{\mathbf{d}}_2\hat{\mathbf{d}}_2 + \hat{\mathbf{d}}_3\hat{\mathbf{d}}_3)$ where I_s is the central principal moment of inertia for a line parallel to the axis of symmetry, and I_t is the central principal moment of inertia for *any* line perpendicular to the axis of symmetry. Thus, one may also write $\underline{\mathbf{I}}^{D_i/D_i^\star} = I_s\hat{\mathbf{c}}_1\hat{\mathbf{c}}_1 + I_t(\hat{\mathbf{c}}_2\hat{\mathbf{c}}_2 + \hat{\mathbf{c}}_3\hat{\mathbf{c}}_3)$. The time derivative in N of ${}^N\mathbf{H}^{D_i/D_i^\star}$ is given by:

$$ \frac{{}^N d\,{}^N\mathbf{H}^{D_i/D_i^\star}}{dt} = \underline{\mathbf{I}}^{D_i/D_i^\star} \cdot \frac{{}^{C_i} d\,{}^N\boldsymbol{\omega}^{D_i}}{dt} + {}^N\boldsymbol{\omega}^{C_i} \times {}^N\mathbf{H}^{D_i/D_i^\star} \qquad (i=1,\ldots,n) \tag{8}$$

$$\begin{aligned}
&= I_s\big[\dot{u}_{6+n+i} + \dot{u}_4\cos\delta_i - \dot{u}_6\sin\delta_i - (u_4\sin\delta_i + u_6\cos\delta_i)u_{6+i}\big]\hat{\mathbf{c}}_1 + \\
&\quad \big[I_t(\dot{u}_5 + \dot{u}_{6+i}) + I_s(u_4\sin\delta_i + u_6\cos\delta_i)u_{6+n+i} \\
&\quad + (I_s - I_t)(u_4\sin\delta_i + u_6\cos\delta_i)(u_4\cos\delta_i - u_6\sin\delta_i)\big]\hat{\mathbf{c}}_2 + \\
&\quad \big[I_t(\dot{u}_4\sin\delta_i + \dot{u}_6\cos\delta_i + u_4u_{6+i}\cos\delta_i - u_6u_{6+i}\sin\delta_i) \\
&\quad - I_su_{6+n+i}(u_5+u_{6+i}) + (I_t - I_s)(u_5+u_{6+i})(u_4\cos\delta_i - u_6\sin\delta_i)\big]\hat{\mathbf{c}}_3
\end{aligned} \tag{9}$$

The position vector $\mathbf{r}^{B^\star P_i}$ from $B^\star$ to a point P_i that is fixed in B and in C_i can be defined as

$$ \mathbf{r}^{B^\star P_i} \triangleq L_{1,i}\hat{\mathbf{b}}_1 + L_{2,i}\hat{\mathbf{b}}_2 + L_{3,i}\hat{\mathbf{b}}_3 \qquad (i=1,\ldots,n) \tag{10}$$

where $L_{1,i}$, $L_{2,i}$, and $L_{3,i}$ are constants. The position vector from P_i to $D_i^\star$, a point fixed in C_i and in D_i, is given by

$$\mathbf{r}^{P_i D_i^\star} = l_i \hat{\mathbf{c}}_1 \qquad (i = 1, \ldots, n) \tag{11}$$

Hence, the position vector $\mathbf{r}^{B^\star D_i^\star}$ from $B^\star$ to $D_i^\star$ is given by

$$\begin{aligned} \mathbf{r}^{B^\star D_i^\star} &= \mathbf{r}^{B^\star P_i} + \mathbf{r}^{P_i D_i^\star} \\ &= L_{1,i}\hat{\mathbf{b}}_1 + L_{2,i}\hat{\mathbf{b}}_2 + L_{3,i}\hat{\mathbf{b}}_3 + l_i\hat{\mathbf{c}}_1 \\ &= (L_{1,i} + l_i\cos\delta_i)\hat{\mathbf{b}}_1 + L_{2,i}\hat{\mathbf{b}}_2 + (L_{3,i} - l_i\sin\delta_i)\hat{\mathbf{b}}_3 \\ &\triangleq k_{1,i}\hat{\mathbf{b}}_1 + k_{2,i}\hat{\mathbf{b}}_2 + k_{3,i}\hat{\mathbf{b}}_3 \qquad (i = 1, \ldots, n) \end{aligned} \tag{12}$$

The velocity ${}^N\mathbf{v}^{D_i^\star}$ of $D_i^\star$ in N is given by

$$\begin{aligned} {}^N\mathbf{v}^{D_i^\star} &= {}^N\mathbf{v}^{B^\star} + {}^N\boldsymbol{\omega}^{B} \times \mathbf{r}^{B^\star P_i} + {}^N\boldsymbol{\omega}^{C_i} \times l_i\hat{\mathbf{c}}_1 \\ &= (u_1 + k_{3,i}u_5 - k_{2,i}u_6 - l_i\sin\delta_i u_{6+i})\hat{\mathbf{b}}_1 + (u_2 - k_{3,i}u_4 + k_{1,i}u_6)\hat{\mathbf{b}}_2 \\ &\quad + (u_3 + k_{2,i}u_4 - k_{1,i}u_5 - l_i\cos\delta_i u_{6+i})\hat{\mathbf{b}}_3 \\ &\triangleq \lambda_{1,i}\hat{\mathbf{b}}_1 + \lambda_{2,i}\hat{\mathbf{b}}_2 + \lambda_{3,i}\hat{\mathbf{b}}_3 \qquad (i = 1, \ldots, n) \end{aligned} \tag{13}$$

The acceleration ${}^N\mathbf{a}^{B^\star}$ of $B^\star$ in N is defined as

$${}^N\mathbf{a}^{B^\star} = \frac{{}^N d\,{}^N\mathbf{v}^{B^\star}}{dt} = \frac{{}^B d\,{}^N\mathbf{v}^{B^\star}}{dt} + {}^N\boldsymbol{\omega}^{B} \times {}^N\mathbf{v}^{B^\star} \tag{14}$$

The acceleration ${}^N\mathbf{a}^{D_i^\star}$ of $D_i^\star$ in N is defined as

$$\begin{aligned} {}^N\mathbf{a}^{D_i^\star} &= \frac{{}^N d\,{}^N\mathbf{v}^{D_i^\star}}{dt} = \frac{{}^B d\,{}^N\mathbf{v}^{D_i^\star}}{dt} + {}^N\boldsymbol{\omega}^{B} \times {}^N\mathbf{v}^{D_i^\star} \qquad (i = 1, \ldots, n) \\ &= \big[\dot{u}_1 + k_{3,i}\dot{u}_5 - l_i\sin\delta_i\dot{u}_{6+i} - \cos\delta_i u_{6+i}l_i(u_5 + u_{6+i}) - k_{2,i}\dot{u}_6 + u_5\lambda_{3,i} - u_6\lambda_{2,i}\big]\hat{\mathbf{b}}_1 + \\ &\quad \big[\dot{u}_2 - k_{3,i}\dot{u}_4 + u_4u_{6+i}l_i\cos\delta_i + k_{1,i}\dot{u}_6 - u_6u_{6+i}l_i\sin\delta_i - u_4\lambda_{3,i} + u_6\lambda_{1,i}\big]\hat{\mathbf{b}}_2 + \\ &\quad \big[\dot{u}_3 - k_{1,i}\dot{u}_5 - l_i\cos\delta_i\dot{u}_{6+i} + \sin\delta_i u_{6+i}l_i(u_5 + u_{6+i}) + k_{2,i}\dot{u}_4 + u_4\lambda_{2,i} - u_5\lambda_{1,i}\big]\hat{\mathbf{b}}_3 \end{aligned} \tag{15}$$

C. Forces and Moments

The set of external forces acting on B is equivalent to a single force $\mathbf{F}_B$ applied at $B^\star$, together with a couple whose torque is $\mathbf{T}_B$. The principal external forces are due to gravity and aerodynamics. Likewise, the set of external forces acting on D_i is equivalent to a single force $\mathbf{F}_i$ applied at $D_i^\star$, together with a couple whose torque is $\mathbf{T}_i$ $(i = 1, \ldots, n)$. The principle external forces acting on each rotor are due to gravity and aerodynamics; thrust resulting from aerodynamic lift applied to the propeller blades is also regarded as an external force. Propeller D_i is made to move relative to B by means of a motor that exerts on D_i a couple whose torque is $\mathbf{M}_i$; according to the law of action and reaction, a couple of torque $-\mathbf{M}_i$ is applied to B. The motor torques are expressed as

$$\mathbf{M}_i = \tau_{6+i}\hat{\mathbf{b}}_2 + \tau_{6+n+i}\hat{\mathbf{c}}_1 \qquad (i = 1, \ldots, n) \tag{16}$$

D. Equations of Motion

Equations of motion obtained using Kane's method are given by

$$\begin{aligned} &{}^N\mathbf{v}_r^{B^\star} \cdot \left(\mathbf{F}_B - m_B\,{}^N\mathbf{a}^{B^\star}\right) + {}^N\boldsymbol{\omega}_r^{B} \cdot \left(\mathbf{T}_B - \sum_{i=1}^{n}\mathbf{M}_i - \frac{{}^N d\,{}^N\mathbf{H}^{B/B^\star}}{dt}\right) \\ &+ \sum_{i=1}^{n}\left[{}^N\mathbf{v}_r^{D_i^\star} \cdot \left(\mathbf{F}_i - m_D\,{}^N\mathbf{a}^{D_i^\star}\right) + {}^N\boldsymbol{\omega}_r^{D_i} \cdot \left(\mathbf{T}_i + \mathbf{M}_i - \frac{{}^N d\,{}^N\mathbf{H}^{D_i/D_i^\star}}{dt}\right)\right] = 0 \quad (r = 1, \ldots, 6 + 2n) \end{aligned} \tag{17}$$

where ${}^N\mathbf{v}_r^{B^\star}$, referred to as the rth partial velocity of $B^\star$ in N (Ref. [15], Sec. 2.14), is simply the vector coefficient of u_r in the right-hand side of Eq. (1). Similarly, ${}^N\boldsymbol{\omega}_r^{B}$ denotes the rth partial angular velocity of

B in N, which is simply the vector coefficient of u_r in the right-hand side of Eq. (2). The partial velocities and partial angular velocities recorded in Table 2 are obtained by inspection of Eqs. (1), (2), (4), and (13). It is worth noting that for $r > 6$ the vectors ${}^N\boldsymbol{\omega}_r^{D_i}$ and ${}^N\mathbf{v}_r^{D_i^\star}$ are $\mathbf{0}$ when r differs from the heading in the final two columns. For example, in connection with the first propeller $i = 1$; ${}^N\boldsymbol{\omega}_7^{D_1} = \hat{\mathbf{b}}_2$, whereas ${}^N\boldsymbol{\omega}_7^{D_2} = \mathbf{0}$, ${}^N\boldsymbol{\omega}_7^{D_3} = \mathbf{0}$, etc. Kane's method yields equations of motion in the general form $[M]\{\dot{u}\} = \{F\}$, where $[M]$ is a symmetric generalized inertia matrix (sometimes referred to as the mass matrix) that, in this case, is dimensioned $(6 + 2n) \times (6 + 2n)$, the column matrix $\{\dot{u}\}$ contains $\dot{u}_1, \ldots, \dot{u}_{6+2n}$, and the column matrix $\{F\}$ is dimensioned $(6 + 2n) \times 1$.

Table 2. Partial velocities and partial angular velocities

r	1	2	3	4	5	6	$6+i$	$6+n+i$
${}^N\mathbf{v}_r^{B^\star}$	$\hat{\mathbf{b}}_1$	$\hat{\mathbf{b}}_2$	$\hat{\mathbf{b}}_3$	$\mathbf{0}$	$\mathbf{0}$	$\mathbf{0}$	$\mathbf{0}$	$\mathbf{0}$
${}^N\boldsymbol{\omega}_r^{B}$	$\mathbf{0}$	$\mathbf{0}$	$\mathbf{0}$	$\hat{\mathbf{b}}_1$	$\hat{\mathbf{b}}_2$	$\hat{\mathbf{b}}_3$	$\mathbf{0}$	$\mathbf{0}$
${}^N\boldsymbol{\omega}_r^{D_i}$	$\mathbf{0}$	$\mathbf{0}$	$\mathbf{0}$	$\hat{\mathbf{b}}_1$	$\hat{\mathbf{b}}_2$	$\hat{\mathbf{b}}_3$	$\hat{\mathbf{b}}_2$	$\hat{\mathbf{c}}_1$
${}^N\mathbf{v}_r^{D_i^\star}$	$\hat{\mathbf{b}}_1$	$\hat{\mathbf{b}}_2$	$\hat{\mathbf{b}}_3$	$-k_{3,i}\hat{\mathbf{b}}_2 + k_{2,i}\hat{\mathbf{b}}_3$	$k_{3,i}\hat{\mathbf{b}}_1 - k_{1,i}\hat{\mathbf{b}}_3$	$-k_{2,i}\hat{\mathbf{b}}_1 + k_{1,i}\hat{\mathbf{b}}_2$	$-l_i\hat{\mathbf{c}}_3$	$\mathbf{0}$

The elements of the generalized inertia matrix $[M]$ are denoted by M_{rs} $(r, s = 1, \ldots, 6+2n)$. The matrix can be partitioned as shown in Eq. (18).

$$M = \begin{bmatrix} M_{R/R} & M_{R/\delta} & M_{R/\phi} \\ M_{\delta/R} & M_{\delta/\delta} & M_{\delta/\phi} \\ M_{\phi/R} & M_{\phi/\delta} & M_{\phi/\phi} \end{bmatrix}_{(6+2n)\times(6+2n)} \tag{18}$$

Explicit expressions for the elements of the generalized inertia matrix partitions are given in Eqs. (19) to (24) , where $m_T = m_B + nm_D$. For brevity, $\sum_{i=1}^{n}$ is replaced by Σ.

$$M_{R/R} = \begin{bmatrix} m_T & 0 & 0 & 0 & m_D\Sigma k_{3,i} & -m_D\Sigma k_{2,i} \\ 0 & m_T & 0 & -m_D\Sigma k_{3,i} & 0 & m_D\Sigma k_{1,i} \\ 0 & 0 & m_T & m_D\Sigma k_{2,i} & -m_D\Sigma k_{1,i} & 0 \\ 0 & -m_D\Sigma k_{3,i} & m_D\Sigma k_{2,i} & M_{44} & M_{45} & M_{46} \\ m_D\Sigma k_{3,i} & 0 & -m_D\Sigma k_{1,i} & M_{54} & M_{55} & M_{56} \\ -m_D\Sigma k_{2,i} & m_D\Sigma k_{1,i} & 0 & M_{64} & M_{65} & M_{66} \end{bmatrix}_{6\times6} \tag{19}$$

where

$$\begin{aligned}
M_{44} &= I_{11} + I_s\Sigma\cos^2\delta_i + I_t\Sigma\sin^2\delta_i + m_D(\Sigma k_{3,i}^2 + \Sigma k_{2,i}^2) \\
M_{54} &= I_{21} - m_D\Sigma k_{1,i}k_{2,i} \\
M_{64} &= I_{31} + (I_t - I_s)\Sigma\cos\delta_i\sin\delta_i - m_D\Sigma k_{1,i}k_{3,i} \\
M_{45} &= I_{12} - m_D\Sigma k_{1,i}k_{2,i} \\
M_{55} &= I_{22} + nI_t + m_D(\Sigma k_{3,i}^2 + \Sigma k_{1,i}^2) \\
M_{65} &= I_{32} - m_D\Sigma k_{2,i}k_{3,i} \\
M_{46} &= I_{13} + (I_t - I_s)\Sigma\cos\delta_i\sin\delta_i - m_D\Sigma k_{1,i}k_{3,i} \\
M_{56} &= I_{23} - m_D\Sigma k_{2,i}k_{3,i} \\
M_{66} &= I_{33} + I_s\Sigma\sin^2\delta_i + I_t\Sigma\cos^2\delta_i + m_D(\Sigma k_{1,i}^2 + \Sigma k_{2,i}^2)
\end{aligned}$$

where $I_{rs} \triangleq \hat{\mathbf{b}}_r \cdot \underline{\mathbf{I}}^{B/B^\star} \cdot \hat{\mathbf{b}}_s$ $(r, s = 1, 2, 3)$ denotes a central moment of inertia of B (when $r = s$) or a central product of inertia of B (when $r \neq s$) for lines parallel to $\hat{\mathbf{b}}_1$, $\hat{\mathbf{b}}_2$, and $\hat{\mathbf{b}}_3$.

$$M_{R/\phi} = {M_{\phi/R}}^T = \begin{bmatrix} 0 & 0 & \dots & 0 \\ 0 & 0 & \dots & 0 \\ 0 & 0 & \dots & 0 \\ I_s \cos\delta_1 & I_s \cos\delta_2 & \dots & I_s \cos\delta_n \\ 0 & 0 & \dots & 0 \\ -I_s \sin\delta_1 & -I_s \sin\delta_2 & \dots & -I_s \sin\delta_n \end{bmatrix}_{6\times n} \tag{20}$$

$$M_{R/\delta} = {M_{\delta/R}}^T = \begin{bmatrix} -m_D l_1 \sin\delta_1 & \dots & -m_D l_n \sin\delta_n \\ 0 & \dots & 0 \\ -m_D l_1 \cos\delta_1 & \dots & -m_D l_n \cos\delta_n \\ -m_D l_1 \cos\delta_1 k_{2,1} & \dots & -m_D l_n \cos\delta_n k_{2,n} \\ I_t - m_D l_1 (k_{3,1}\sin\delta_1 - k_{1,1}\cos\delta_1) & \dots & I_t - m_D l_n (k_{3,n}\sin\delta_n - k_{1,n}\cos\delta_n) \\ m_D l_1 k_{2,1} \sin\delta_1 & \dots & m_D l_n k_{2,n} \sin\delta_n \end{bmatrix}_{6\times n} \tag{21}$$

$$M_{\phi/\phi} = \begin{bmatrix} I_s & \dots & 0 \\ \vdots & \ddots & \vdots \\ 0 & \dots & I_s \end{bmatrix}_{n\times n} \tag{22}$$

$$M_{\phi/\delta} = {M_{\delta/\phi}}^T = \begin{bmatrix} 0 & \dots & 0 \\ \vdots & \ddots & \vdots \\ 0 & \dots & 0 \end{bmatrix}_{n\times n} \tag{23}$$

$$M_{\delta/\delta} = \begin{bmatrix} I_t + m_D {l_1}^2 & \dots & 0 \\ \vdots & \ddots & \vdots \\ 0 & \dots & I_t + m_D {l_n}^2 \end{bmatrix}_{n\times n} \tag{24}$$

Elements of the matrix $\{F\}_{(6+2n)\times 1}$ are shown in Eqs. (25)–(32).

$$F_1 = -m_B(u_5 u_3 - u_6 u_2) - m_D \Sigma \left[-u_{6+i}(u_5 + u_{6+i}) l_i \cos\delta_i + u_5 \lambda_{3,i} - u_6 \lambda_{2,i}\right] + \hat{\mathbf{b}}_1 \cdot (\mathbf{F}_B + \Sigma \mathbf{F}_i) \tag{25}$$

$$F_2 = -m_B(-u_4 u_3 + u_6 u_1) - m_D \Sigma \left[u_{6+i} l_i (u_4 \cos\delta_i - u_6 \sin\delta_i) - u_4 \lambda_{3,i} + u_6 \lambda_{1,i}\right] + \hat{\mathbf{b}}_2 \cdot (\mathbf{F}_B + \Sigma \mathbf{F}_i) \tag{26}$$

$$F_3 = -m_B(u_4 u_2 - u_5 u_1) - m_D \Sigma \left[u_{6+i}(u_5 + u_{6+i}) l_i \sin\delta_i + u_4 \lambda_{2,i} - u_5 \lambda_{1,i}\right] + \hat{\mathbf{b}}_3 \cdot (\mathbf{F}_B + \Sigma \mathbf{F}_i) \tag{27}$$

$$\begin{aligned} F_4 = & -({}^N\boldsymbol{\omega}^B \times \underline{\mathbf{I}}^{B/B^\star} \cdot {}^N\boldsymbol{\omega}^B) \cdot \hat{\mathbf{b}}_1 + I_s \Sigma \cos\delta_i u_{6+i}(u_4 \sin\delta_i + u_6 \cos\delta_i) \\ & - I_t \Sigma \sin\delta_i u_{6+i}(u_4 \cos\delta_i - u_6 \sin\delta_i) + I_s \Sigma \sin\delta_i u_{6+n+i}(u_5 + u_{6+i}) \\ & - (I_t - I_s)\Sigma \sin\delta_i (u_5 + u_{6+i})(u_4 \cos\delta_i - u_6 \sin\delta_i) \\ & + m_D \Sigma k_{3,i} \left[u_{6+i} l_i (u_4 \cos\delta_i - u_6 \sin\delta_i) - u_4 \lambda_{3,i} + u_6 \lambda_{1,i}\right] \\ & - m_D \Sigma k_{2,i} \left[u_{6+i}(u_5 + u_{6+i}) l_i \sin\delta_i + u_4 \lambda_{2,i} - u_5 \lambda_{1,i}\right] + \hat{\mathbf{b}}_1 \cdot (\mathbf{T}_B + \Sigma \mathbf{T}_i) \\ & + \Sigma (k_{2,i} \hat{\mathbf{b}}_3 - k_{3,i} \hat{\mathbf{b}}_2) \cdot \mathbf{F}_i \end{aligned} \tag{28}$$

$$
\begin{aligned}
F_5 = &-({}^N\boldsymbol{\omega}^B \times \underline{\mathbf{I}}^{B/B^\star} \cdot {}^N\boldsymbol{\omega}^B) \cdot \hat{\mathbf{b}}_2 - I_s \Sigma u_{6+n+i}(u_4 \sin\delta_i + u_6 \cos\delta_i) \\
&- (I_s - I_t)(u_4 \sin\delta_i + u_6 \cos\delta_i)(u_4 \cos\delta_i - u_6 \sin\delta_i) \\
&- m_D \Sigma k_{3,i} \left[-u_{6+i}(u_5 + u_{6+i}) l_i \cos\delta_i + u_5 \lambda_{3,i} - u_6 \lambda_{2,i}\right] \\
&+ m_D \Sigma k_{1,i} \left[u_{6+i}(u_5 + u_{6+i}) l_i \sin\delta_i + u_4 \lambda_{2,i} - u_5 \lambda_{1,i}\right] + \hat{\mathbf{b}}_2 \cdot (\mathbf{T}_B + \Sigma \mathbf{T}_i) \\
&+ \Sigma(k_{3,i}\hat{\mathbf{b}}_1 - k_{1,i}\hat{\mathbf{b}}_3) \cdot \mathbf{F}_i
\end{aligned} \tag{29}
$$

$$
\begin{aligned}
F_6 = &-({}^N\boldsymbol{\omega}^B \times \underline{\mathbf{I}}^{B/B^\star} \cdot {}^N\boldsymbol{\omega}^B) \cdot \hat{\mathbf{b}}_3 - I_s \Sigma \sin\delta_i u_{6+i}(u_4 \sin\delta_i + u_6 \cos\delta_i) \\
&- I_t \Sigma \cos\delta_i u_{6+i}(u_4 \cos\delta_i - u_6 \sin\delta_i) + I_s \Sigma \cos\delta_i u_{6+n+i}(u_5 + u_{6+i}) \\
&- (I_t - I_s)\Sigma \cos\delta_i (u_5 + u_{6+i})(u_4 \cos\delta_i - u_6 \sin\delta_i) \\
&+ m_D \Sigma k_{2,i} \left[-u_{6+i}(u_5 + u_{6+i}) l_i \cos\delta_i + u_5 \lambda_{3,i} - u_6 \lambda_{2,i}\right] \\
&- m_D \Sigma k_{1,i} \left[u_{6+i} l_i (u_4 \cos\delta_i - u_6 \sin\delta_i) - u_4 \lambda_{3,i} + u_6 \lambda_{1,i}\right] + \hat{\mathbf{b}}_3 \cdot (\mathbf{T}_B + \Sigma \mathbf{T}_i) \\
&+ \Sigma(k_{1,i}\hat{\mathbf{b}}_2 - k_{2,i}\hat{\mathbf{b}}_1) \cdot \mathbf{F}_i
\end{aligned} \tag{30}
$$

$$
\begin{aligned}
F_{6+i} = &-(u_4 \sin\delta_i + u_6 \cos\delta_i)\left[I_s u_{6+n+i} + (I_s - I_t)(u_4 \cos\delta_i - u_6 \sin\delta_i)\right] \\
&+ m_D l_i \sin\delta_i \left(u_5 \lambda_{3,i} - u_6 \lambda_{2,i}\right) + m_D l_i \cos\delta_i \left(u_4 \lambda_{2,i} - u_5 \lambda_{1,i}\right) + \tau_{6+i} + \hat{\mathbf{b}}_2 \cdot \mathbf{T}_i \\
&- l_i \hat{\mathbf{c}}_3 \cdot \mathbf{F}_i
\end{aligned} \tag{31}
$$

$$
F_{6+n+i} = I_s u_{6+i}(u_4 \sin\delta_i + u_6 \cos\delta_i) + \tau_{6+n+i} + \hat{\mathbf{c}}_1 \cdot \mathbf{T}_i \tag{32}
$$

E. System Angular Momentum and Kinetic Energy

Let S denote the multibody system made up of B and $D_1, \ldots, D_n$. The angular momentum ${}^N\mathbf{H}^{S/S^\star}$ in N of S with respect to $S^\star$, the system mass center, is given by

$$
\begin{aligned}
{}^N\mathbf{H}^{S/S^\star} &= \underline{\mathbf{I}}^{B/B^\star} \cdot {}^N\boldsymbol{\omega}^B + m_B \mathbf{r}^{S^\star B^\star} \times {}^N\mathbf{v}^{B^\star} + \sum_{i=1}^{n} \left(\underline{\mathbf{I}}^{D_i/D_i^\star} \cdot {}^N\boldsymbol{\omega}^{D_i} + m_D\, \mathbf{r}^{S^\star D_i^\star} \times {}^N\mathbf{v}^{D_i^\star}\right) \\
&= \underline{\mathbf{I}}^{B/B^\star} \cdot {}^N\boldsymbol{\omega}^B + \sum_{i=1}^{N} \left[\underline{\mathbf{I}}^{D_i/D_i^\star} \cdot {}^N\boldsymbol{\omega}^{D_i} + m_D\, \mathbf{r}^{S^\star D_i^\star} \times \left({}^N\boldsymbol{\omega}^B \times \mathbf{r}^{B^\star P_i} + {}^N\boldsymbol{\omega}^{C_i} \times l_i \hat{\mathbf{c}}_1\right)\right]
\end{aligned} \tag{33}
$$

According to the angular momentum principle, ${}^N\mathbf{H}^{S/S^\star}$ has constant direction in N and constant magnitude when the moment about $S^\star$ of external forces vanishes.

The kinetic energy K of S in N is given by

$$
K = \frac{1}{2}\left[m_B\, {}^N\mathbf{v}^{B^\star} \cdot {}^N\mathbf{v}^{B^\star} + {}^N\boldsymbol{\omega}^B \cdot \underline{\mathbf{I}}^{B/B^\star} \cdot {}^N\boldsymbol{\omega}^B + \sum_{i=1}^{n}\left(m_D\, {}^N\mathbf{v}^{D_i^\star} \cdot {}^N\mathbf{v}^{D_i^\star} + {}^N\boldsymbol{\omega}^{D_i} \cdot \underline{\mathbf{I}}^{D_i/D_i^\star} \cdot {}^N\boldsymbol{\omega}^{D_i}\right)\right] \tag{34}
$$

Mechanical energy E is the sum of K and V, a potential energy of S in N. If K is a homogeneous quadratic function of $u_1, \ldots, u_{6+2n}$ then E is a constant (Ref. [16], Sec. 9.2). It can be shown that K is expressed as

$$
\begin{aligned}
K = \frac{1}{2}\Bigg\{ &m_B({u_1}^2 + {u_2}^2 + {u_3}^2) + \sum_{r=1}^{3}\sum_{s=1}^{3} I_{rs} u_{r+3} u_{s+3} + \sum_{i=1}^{n}\Big[m_D[(u_1 + k_{3,i}u_5 - k_{2,i}u_6 - l_i \sin\delta_i u_{6+i})^2 \\
&+ (u_2 - k_{3,i}u_4 + k_{1,i}u_6)^2 + (u_3 + k_{2,i}u_4 - k_{1,i}u_5 - l_i \cos\delta_i u_{6+i})^2] \\
&+ I_s(u_4 \cos\delta_i - u_6 \sin\delta_i + u_{6+n+i})^2 + I_t(u_5 + u_{6+i})^2 + I_t(u_4 \sin\delta_i + u_6 \cos\delta_i)^2\Big]\Bigg\}
\end{aligned} \tag{35}
$$

Thus, K is seen to be a homogeneous quadratic function of the motion variables. V vanishes in the absence of external forces, external moments, and motor torques, in which case K is constant.

III. Simulation Results

The intent of the paper is to present multibody dynamical equations of motion for a generic tilt-rotor aircraft, perform certain checks on the validity of the equations, and contrast numerical solutions of the equations with those obtained from the conventional approach in which the aircraft is modeled as a single rigid body. In what follows the equations are applied to a specific notional vehicle with four rotors, such as the one shown in Fig. 1, and solved numerically for two cases. The first case constitutes a check of the validity of the equations and the numerical solutions. The second case involves motions of the vehicle that are reflective of realistic flight operations. Parameters for the notional vehicle are provided in Tables 3 and 4. Inertia matrices for B and D are provided in Eqs. (36) and (37), respectively.

Table 3. System parameters

Parameter	Value
m_B	2176 kg
m_D	118 kg
l	1 m

Table 4. Propeller locations

i	$L_{1,i}$ (m)	$L_{2,i}$ (m)	$L_{3,i}$ (m)
1	0.5	−5.5	−0.25
2	0.5	5.5	−0.25
3	−2.5	−2.5	−0.5
4	−2.5	2.5	−0.5

$$I_B = \begin{bmatrix} 74110 & 0 & 0 \\ 0 & 6780 & 0 \\ 0 & 0 & 74529 \end{bmatrix} \text{kg-m}^2 \tag{36}$$

$$I_D = \begin{bmatrix} 137 & 0 & 0 \\ 0 & 69 & 0 \\ 0 & 0 & 69 \end{bmatrix} \text{kg-m}^2 \tag{37}$$

A. Case 1: System Response to Initial Conditions

In this example the response of the multibody system to a set of initial conditions is shown. Gravity, thrust forces produced by the propellers, and motor torques are absent. That is to say, $\mathbf{F}_B$, $\mathbf{T}_B$, $\mathbf{F}_i$, $\mathbf{T}_i$, and $\mathbf{M}_i$ $(i = 1, 2, 3, 4)$ are all equal to the vector $\mathbf{0}$. The values of K and ${}^N\mathbf{H}^{S/S^\star}$ are calculated at each step in the numerical solution of the equations of motion in order to provide confidence that the equations are derived correctly and the numerical solution is accurate to machine precision. A numerical solution of the equations of motion is obtained for the following values of the motion variables at $t = 0$: $u_1 = 100$ m/s, $u_2 = 0$ m/s, $u_3 = 0$ m/s, $u_4 = -2.865$ deg/s, $u_5 = 5.73$ deg/s, $u_6 = 1.146$ deg/s, $u_7 = u_8 = u_9 = u_{10} = 5.73$ deg/s, $u_{11} = -u_{12} = -5443.5$ deg/s, $u_{13} = -u_{14} = 5443.5$ deg/s, $\delta_i = 0$ deg $(i = 1, \ldots, 4)$. Figures 2–4 show the vehicle and propeller states along with the kinetic energy of the system and the magnitude of the system angular momentum. The three components of ${}^N\mathbf{H}^{S/S^\star}$ are shown in Fig. 5. In the absence of external moments, the magnitude of the system angular moment is constant and its direction is fixed in N. For comparison, solutions obtained with the single-rigid-body approach are co-plotted and shown in blue. In that approach, m_B is adjusted to account for the mass of the propellers, and I_B is adjusted to include parallel-axis terms associated with treating the propellers as particles. (The propeller moments of inertia

in Eq. 37 are ignored, which is why single-rigid-body values differ from the multibody values in Figs. 4 and 5.) Although the multibody system in actual flight is not likely to undergo motions depicted in Fig. 2, the comparison nevertheless demonstrates that a single-rigid-body dynamic model fails to reflect dynamic coupling that must be present in the physical system. In Fig. 3 it is worth noting that there are significant departures of the gimbal angles from their initial values because there are no motor torques present.

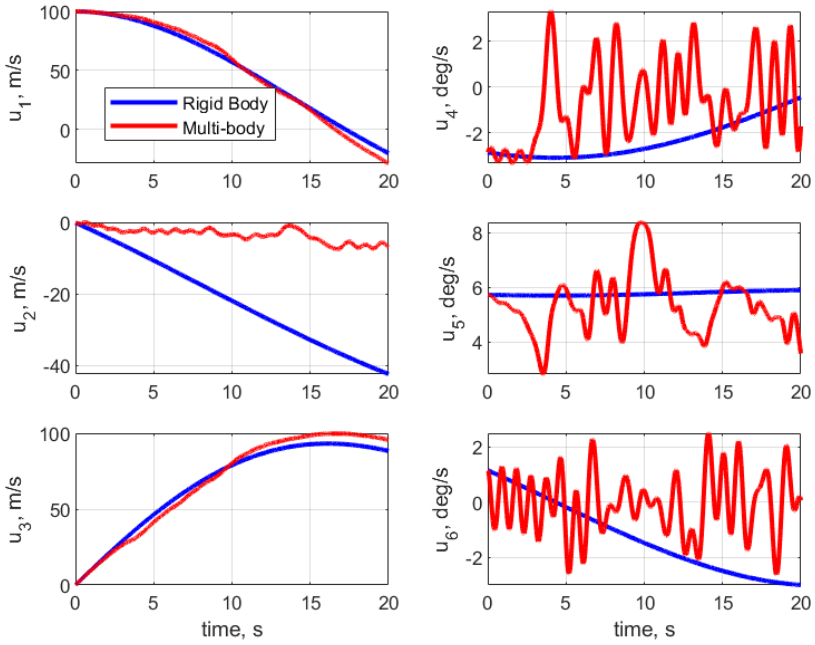

Figure 2. Vehicle rigid body states, case 1.

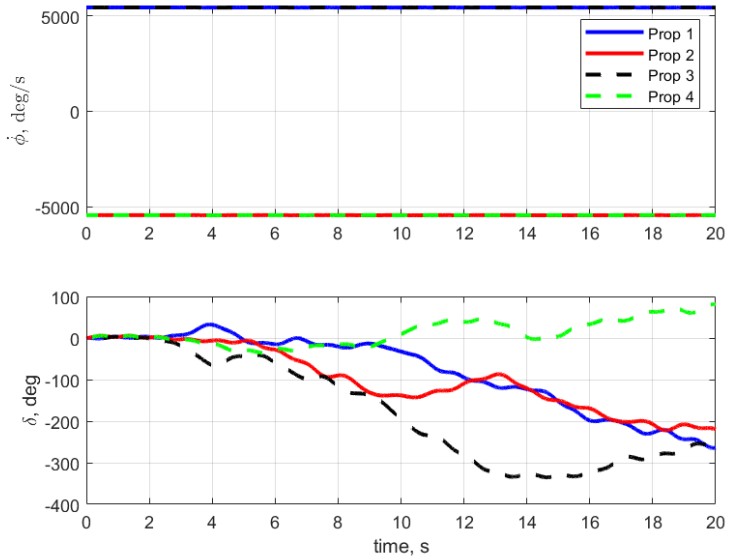

Figure 3. Propeller states, case 1.

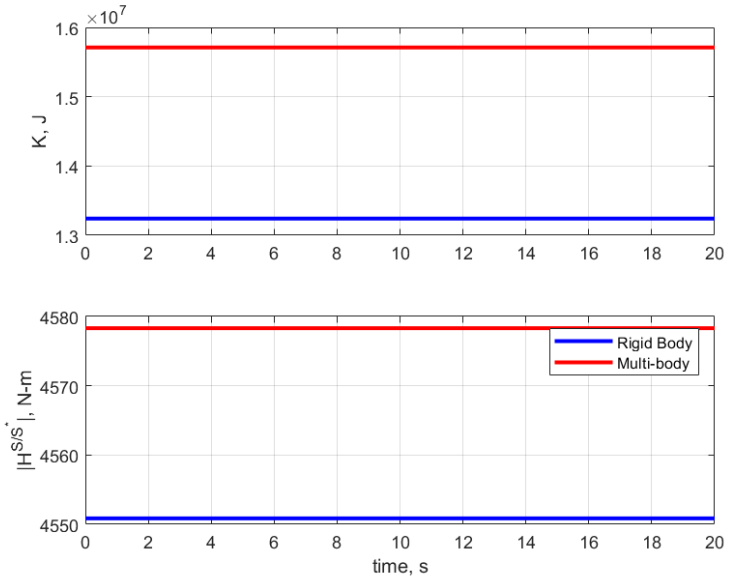

Figure 4. System kinetic energy and magnitude of system angular momentum, case 1.

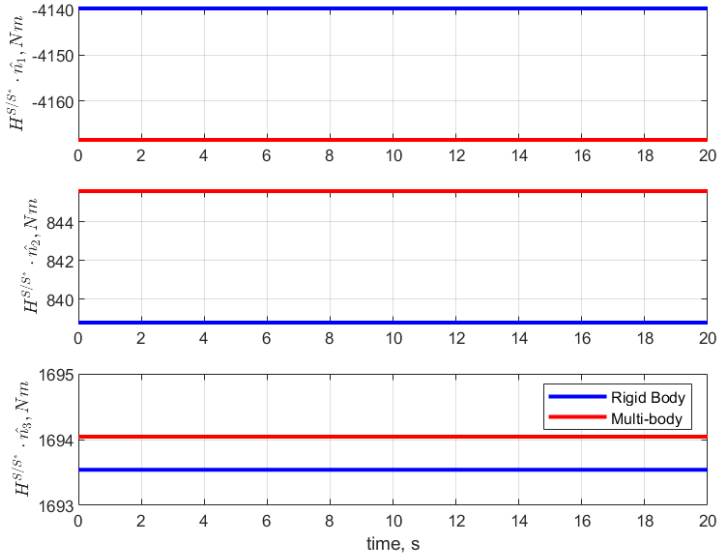

Figure 5. System angular momentum in N, case 1.

B. Case 2: System Response to Open Loop Gimbal Commands

The second example begins with the vehicle hovering and $\delta_i = 90$ deg $(i = 1, \ldots, 4)$. Initial values of the motion variables are $u_1 = u_2 = u_3 = 0$ m/s, $u_4 = u_5 = u_6 = 0$ deg/s, $u_7 = u_8 = u_9 = u_{10} = 0$ deg/s, $u_{11} = -u_{12} = 18622$ deg/s, and $u_{13} = -u_{14} = 5433.5$ deg/s. At $t = 5$ s an open loop command is issued to gimbal all four nacelles forward by means of motor torques $\tau_{6+i}\hat{\mathbf{b}}_2$, which results in $\dot{\delta}_i = -2.86$ deg/s. At $t = 10$ s the nacelles are commanded to move back to $\delta_i = 90$ deg at a rate of $\dot{\delta}_i = 2.86$ deg/s. In the final 5 s the vehicle is in trimmed level flight with a constant forward speed. The thrust produced by each propeller is taken to be equal to the product of a constant and the propeller speed $\dot{\phi}_i$. At each time step commands are issued to adjust the thrust of each propeller by applying motor torques $\tau_{6+n+i}\hat{\mathbf{c}}_1$ such that

the magnitude of the projection of the resultant thrust on to $\hat{\mathbf{b}}_3$ is equal to the vehicle's weight, and the resultant external moment about the vehicle system mass center is zero.

Figures 6 and 7 show the vehicle and propeller states. For comparison, solutions obtained with the single-rigid-body approach are co-plotted and shown in blue. It is apparent in the time history of u_5 (pitch rate) in the multibody results that, in keeping with the law of action and reaction, the fuselage pitches up when the nacelles pitch down, and vice versa. The pitch attitude reaches a maximum value of 1.25 deg after the first maneuver. This is analogous to the "tail-wags-dog" behavior of a thrust-vector controlled launch vehicle discussed in Ref. [17]. The single-rigid-body approach does not predict the pitching motion of the fuselage or the multibody time history of u_3, and yields a different final forward speed of the fuselage as seen in the time histories of u_1. The small changes in the angular speeds of propellers 1 and 2 observed in Fig. 7 are reflective of the thrusts required to trim the vehicle at each time step.

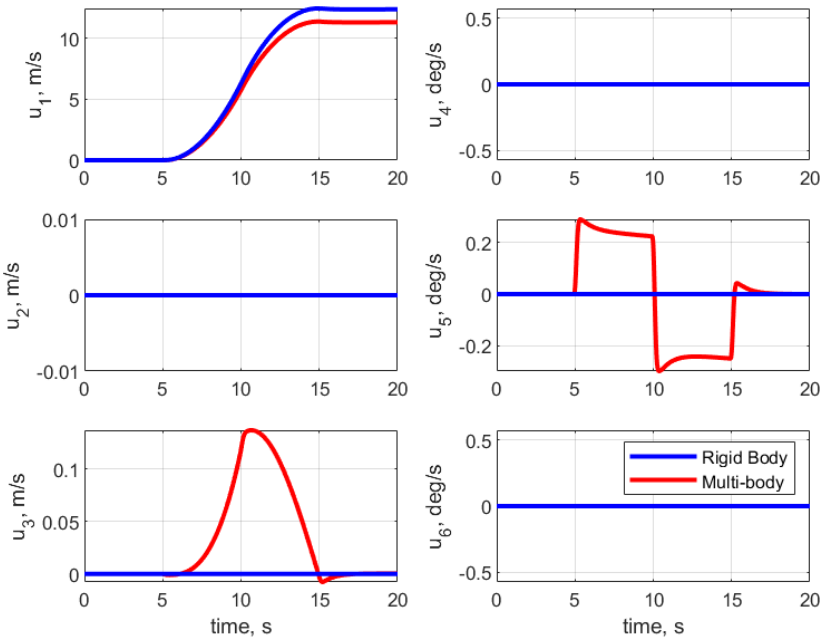

Figure 6. Vehicle rigid body states, case 2.

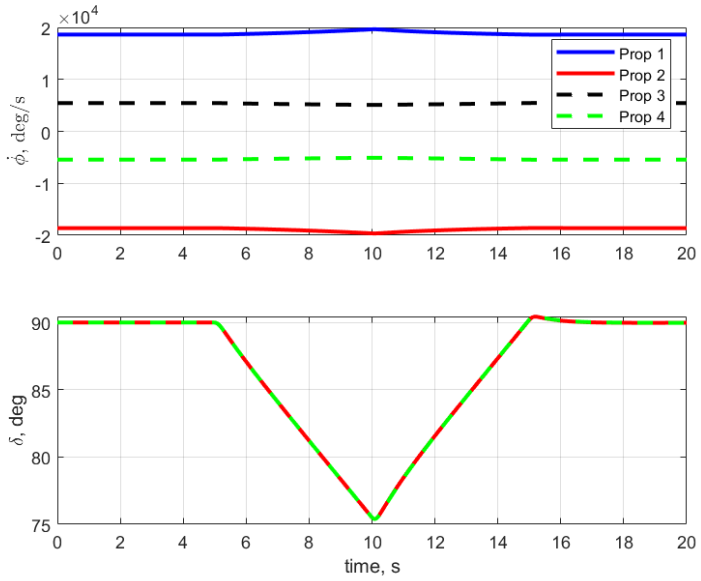

Figure 7. Propeller states, case 2.

IV. Conclusion

Kane's method is used to derive explicit analytical dynamical equations of motion for a multibody model of a generic tilt-rotor aircraft. Nacelles are permitted to move independently of each other, as are the rotors. The number of equations, which is equal to the number of degrees of freedom, is therefore $6 + 2n$, where n is the number of rotors in the model. The equations are applied to a four-rotor configuration and solved numerically for two cases, the first of which serves as a check of the validity of the equations and numerical solutions. Results obtained with the multibody equations are compared to those produced by the traditional single-body approach. The latter approach fails to identify important motions of the system that are made evident when using the higher fidelity, multibody approach. A multibody model is recommended when the mass and inertia of appendages are significant compared to those of the fuselage, or appendages are moving at high speeds relative to the fuselage, or large motor torques are involved.

Acknowledgments

The authors would like to thank Dr. Jared Grauer, Michael Acheson, and Jacob Cook for their technical reviews of a draft of this paper and for sharing their insights with us.

References

[1]Simmons, B. M., and Murphy, P. C., "Wind Tunnel-Based Aerodynamic Model Identification for a Tilt-Wing, Distributed Electric Propulsion Aircraft," *AIAA SciTech 2021 Forum*, AIAA Paper 2021-1298, Jan. 2021.
https://doi.org/10.2514/6.2021-1298

[2]Rothhaar, P. M., Murphy, P. C., Bacon, B. J., Gregory, I. M., Grauer, J. A., Busan, R. C., and Croom, M. A., "NASA Langley Distributed Propulsion VTOL Tilt-Wing Aircraft Testing, Modeling, Simulation, Control, and Flight Test Development," *14th AIAA Aviation Technology, Integration, and Operations Conference*, AIAA Paper 2014-2999, June 2014.
https://doi.org/10.2514/6.2014-2999

[3]"Joby Aviation" https://transportup.com/joby-aviation/ [accessed 14 May, 2021].

[4]Rosenstein, H., and Clark, R., "Aerodynamic Development of the V-22 Tilt Rotor," *AIAA/AHS/ASEE Aircraft Systems, Design, and Technology Meeting*, AIAA Paper 86-2678, Oct. 1986.
https://doi.org/10.2514/6.1986-2678

[5]Maisel, D. M., Guilianetti, J. D., and Dugan, C. D., *The History of the XV-15 Tilt Rotor Research Aircraft: From Concept to Flight*, NASA SP 2000-4517, Washington D.C., 2000.

[6]Rosenstein, H., McVeigh, M., and Mollenkof, P., *Mathematical Model for a Real Time Simulation of a Tilt Rotor Aircraft*, NASA CR-114601, 1973.

[7]Ferguson, W. S., *A Mathematical Model for Real Time Flight Simulation of a Generic Tilt-Rotor Aircraft*, NASA CR-166536, 1988.

[8]Aba, A., Barra, F., Capone, P., and Guglieri, G., "Mathematical Modelling of Gimballed Tilt-Rotors for Real-Time Flight Simulation," *Aerospace*, Vol. 7, No. 9, 2020.
https://doi.org/10.3390/aerospace7090124

[9]Ghiringhelli, G., Masarati, P., Mantegazza, P., and Nixon, W. M., "Multi-Body Analysis of a Tiltrotor Configuration," *Nonlinear Dynamics*, Vol. 19., 1999, pp. 333–357.
https://doi.org/10.1023/A:1008386219934

[10]Mottaboni, M., Masarati, P., Quaranta, G., and Mantegazza, P., "Multibody Simulation of Integrated Tiltrotor Flight Mechanics, Aeroelasticity and Control," *Journal of Guidance, Control, and Dynamics*, Vol. 35, No. 5, 2012, pp. 1391–1405.
https://doi.org/10.2514/1.57309

[11]Miller, M., and Narkiewicz, J., "Tiltrotor Modeling for Simulation in Various Flight Conditions," *Journal of Theoretical and Applied Mechanics*, Vol. 44, No. 4, 2006, pp. 881–906.

[12]Haixu, L., Xiangju, Q., and Weijun, W., "Multi-body Motion Modeling and Simulation for Tilt Rotor Aircraft," *Chinese Journal of Aeronautics* Vol. 23, No. 4, 2010, pp. 415–422.
https://doi.org/10.1016/S1000-9361(09)60236-3

[13]Su, J., Su, C., Xu, S., and Yang, X., "A Multibody Model of Tilt-Rotor Aircraft Based on Kane's Method," *International Journal of Aerospace Engineering*, Vol. 2019, Article ID 9396352.
https://doi.org/10.1155/2019/9396352

[14]https://rotorcraft.arc.nasa.gov/Research/Programs/LCTR.html [accessed 10 May, 2021].

[15]Kane, T. R., and Levinson, D. A., *Dynamics: Theory and Applications*, McGraw-Hill, New York, 1985, Chaps. 6, 7.

[16]Roithmayr, C. M., and Hodges, D. H., *Dynamics: Theory and Application of Kane's Method*, Cambridge University Press, New York, 2016, Chaps. 7, 9.

[17]Orr, J. "A Flight Dynamics Model for a Multi-Actuated Flexible Rocket Vehicle," *AIAA Atmospheric Flight Mechanics Conference*, AIAA Paper 2011-6563, August, 2011.
https://doi.org/10.2514/6.2011-6563